New Results on Selection Diversity

Elisabeth A. Neasmith, *Member IEEE*, and Norman C. Beaulieu, *Senior Member, IEEE*

***Abstract*— The performances of selection diversity receiver structures in a slow flat Rayleigh-fading environment are assessed. A number of new and interesting results are obtained. Binary digital signaling using noncoherent frequency-shift keying (NCFSK), differential phase-shift keying (DPSK), coherent phase-shift keying (CPSK), and coherent frequency-shift keying (CFSK) is considered. The traditional analysis (the Traditional Selection Diversity Model) of a selection diversity system is based on choosing the branch with the largest signal-*to*-noise (SNR) power ratio while assuming that the noise power is constant across all branches. However, many practical selection systems choose the branch based on a largest signal-*plus*-noise ($S+N$ selection) sample of a filter output. This paper comprises accurate analyses of such $S+N$ selection systems. Results show that $S+N$ selection systems perform better than predicted by the Traditional Selection Diversity Model. This is because the former includes the statistical nature of the noise, whereas the latter does not. The performance difference between the two models increases as the number of diversity branches increases. For each of DPSK and CPSK, the dual diversity equal gain (EG) combining and $S+N$ selection systems perform identically. For each of NCFSK and CFSK, receiver structures which are equivalent when there is no diversity perform differently in a diversity environment. Certain dual diversity $S+N$ selection systems give the same performances as EG combining or square law combining. The results are contingent upon perfect cophasing for the EG combining. In systems where estimates of the combining carrier phases contain noise, $S+N$ selection outperforms EG combining for dual diversity.**

***Index Terms*— Combining techniques, diversity, fading channels.**

I. Introduction

DIVERSITY is a well-known technique used to compensate for the unacceptable signal fades experienced on wireless communication channels. This paper assesses the performance of selection diversity receiver structures in a slow frequency-nonselective Rayleigh-fading and additive white Gaussian noise (AWGN) environment. Binary digital signaling using noncoherent frequency-shift keying (NCFSK), differential phase-shift keying (DPSK), coherent phase-shift keying (CPSK), and coherent frequency-shift keying (CFSK) are considered. The results challenge traditional thinking.

Paper approved by O. Andrisano, the Editor for Modulation of the IEEE Communications Society. Manuscript received November 15, 1996; revised April 15, 1997, October 15, 1997, and February 15, 1998. This paper was presented in part at WIRELESS'96, Calgary, Alta., Canada, July 9, 1996.

E. A. Neasmith is with the Department of National Defence, Ottawa, Ont. K1A 0K2, Canada.

N. C. Beaulieu is with the Department of Electrical and Computer Engineering, Queen's University, Kingston, Ont. K7L 3N6, Canada (e-mail: normb@quidnee.ee.queensu.ca).

Publisher Item Identifier S 0090-6778(98)03863-X.

The traditional analysis of a selection diversity system (hereafter referred to as the Traditional Selection Diversity Model) specifies that of L diversity branches $j=1,2,\cdots,L$, the one providing the largest signal-to-noise (S/N) power ratio (SNR) be selected for data recovery. For binary NCFSK signaling in a Rayleigh-fading environment, Pierce [1] provides an expression for the L-branch average bit-error rate (BER) using the Traditional Selection Diversity Model. It is computed by averaging the time-invariant (static) channel-error rate $P(\gamma)$ over the probability density function (pdf) $f(\gamma)$ of the largest SNR $\gamma=\alpha^2\cdot\gamma_b$ of the L branches, where α is the largest (best) fading parameter of the α_j, $j=1,2,\cdots,L$ and $\gamma_b=E_b/N_o$ is the SNR per bit. The Traditional Selection Diversity Model establishes the average BER as [1]

$$P(e)_{\mathrm{NCFSK_{Trad}}}=\frac{1}{2}\cdot\prod_{i=1}^{L}\frac{i}{i+\overline{\gamma}_b/2}. \tag{1}$$

In (1) $\overline{\gamma}_b=\gamma_b\cdot E\{\alpha_j^2\}$ is the average SNR per bit and $E\{\alpha_j^2\}$ is the mean value of the square fading parameter, assumed to be the same on all branches $j=1,2,\cdots,L$ and independent of j.

Note that this analysis, which is often cited [2], uses the pdf which is actually that of the largest signal S independent of the noise. This is appropriate only if, in measuring the largest SNR, the average noise power, computed as

$$\overline{n^2(t)}=\frac{1}{\tau}\int_0^{\tau}n^2(t)\,dt \tag{2}$$

is taken over a sufficiently long time τ such that it may be considered as a constant across all branches. In other words, in cases where τ is long compared to the variability of the noise power, choosing the largest S/N is equivalent to choosing the largest S so that use of the above-mentioned pdf in the analyses in [1] and [2] is accurate.

For practical implementations, however, measurement of SNR may be difficult or expensive, especially for high signaling rates. For this reason, the branch with the largest signal-*plus*-noise is often chosen. We use $S+N$ to denote a signal-plus-noise sample (i.e., not a power measurement). Historical justification for the extensive use of an SNR analysis (the Traditional Selection Diversity Model) to describe the performance of $S+N$ selection systems stems from the idea that any branch which has the largest SNR must also have the largest sum of signal power and noise power if the noise power is taken to be a constant on all branches [3]. When physically realizing $S+N$ selection, though, by sampling the

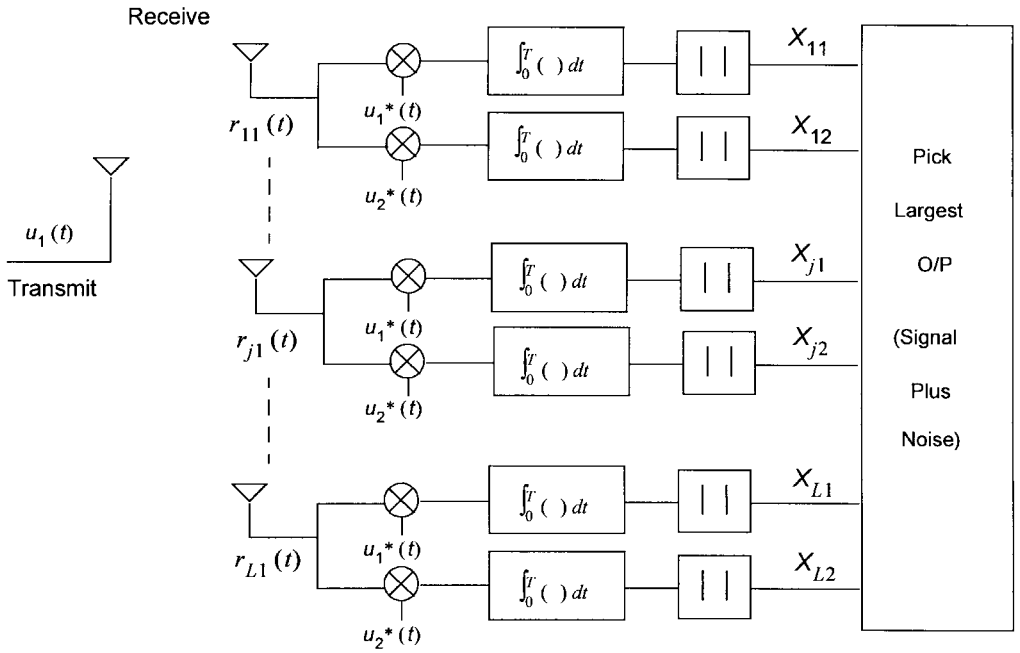

Fig. 1. Binary NCFSK $S + N$ Selection Receiver Model 1 showing $u_1(t)$ being transmitted for analysis purposes.

output of a matched filter, the noise is a random variable. Thus, it is inexact to specify the performance of $S + N$ selection systems using a constant noise analysis. In fact, intuitively one would expect $S + N$ selection to yield a better error performance than that predicted by the Traditional Selection Diversity Model because with the former system there is opportunity for at least one sample to be better (less noisy) than the average of the samples. This is confirmed in [4] and [5], although neither reference offers an explanation for the observed results.

This paper provides exact analyses of $S + N$ selection systems and explains the significance of the results by comparing the observed performances to the performances of other common combining techniques. As the signaling scheme most commonly employed with selection diversity, NCFSK is considered first with specific receiver structures analyzed in Section II and performance results provided in Section III. These analyses and results are specific to binary orthogonal signaling. In Section IV binary antipodal DPSK is presented as a variant of the above-mentioned NCFSK analyses and results. Finally, the coherent signaling schemes CPSK and CFSK are addressed in Section V. Conclusions follow in Section VI.

II. Binary NCFSK System Models and Analyses

In this section we examine three binary orthogonal NCFSK $S+N$ selection diversity receiver structures: $S+N$ Selection Receiver Models 1, 2, and 3. These structures have the same performance when the traditional S/N analysis is used to predict their performances [see (1)]. As will be shown, the structures have different performances when an $S + N$ selection analysis specific to each receiver structure is implemented. In all cases, symbol synchronization is assumed.

A. S + N Selection Receiver Model 1

The $S + N$ Selection Receiver Model 1, depicted in Fig. 1, has been analyzed previously in [4] but is covered briefly here for clarity. Note that of the possible (low-pass equivalent) transmissions in a binary orthogonal system $u_1(t)$ and $u_2(t)$, it has been (arbitrarily) chosen to transmit $u_1(t)$ to analyze the system. The output statistics from each branch are $X_{j1} = |2\alpha_j + Y_{j1}|$ and $X_{j2} = |Y_{j2}|$, where the complex Gaussian random variables Y_{jm}, $m = 1, 2$ are independent and identically distributed (i.i.d.) with zero mean and variance $4/\overline{\gamma}_b$. The average BER for binary signaling $(M = 2)$ is expressed as [4]

$$\begin{aligned} P(e)_{\mathrm{NCFSK}_{S+N\,\mathrm{Model\,1}}} &= \Pr[\max\{X_{j1} < \max\{X_{j2}\}] \\ &= L \cdot \prod_{j=1}^{L}\Big[\Pr(X_{j1} < X_{12})\Big] \cdot \prod_{j=2}^{L}\Big[\Pr(X_{j2} < X_{12}\Big] \\ &= L \cdot \int_0^\infty [F_{X_{11}}(x)]^L \cdot [F_{X_{22}}(x)]^{L-1} \cdot f_{X_{12}}(x)\,dx \end{aligned} \quad (3)$$

where $F_{X_{11}}(x)$ and $F_{X_{22}}(x)$ are the respective cumulative distribution functions (cdf's) of the random variables X_{11} and X_{22}, and $f_{X_{12}}(x)$ is the pdf of the random variable X_{12}. The solution to (3) is [4]

$$P(e)_{\mathrm{NCFSK}_{S+N\,\mathrm{Model\,1}}} = \sum_{j=0}^{L}(-1)^j \binom{L}{j} \prod_{k=1}^{L} \frac{k}{k + j/(1+\overline{\gamma}_b)} \quad (4)$$

where $\overline{\gamma}_b$ was defined in the introduction.

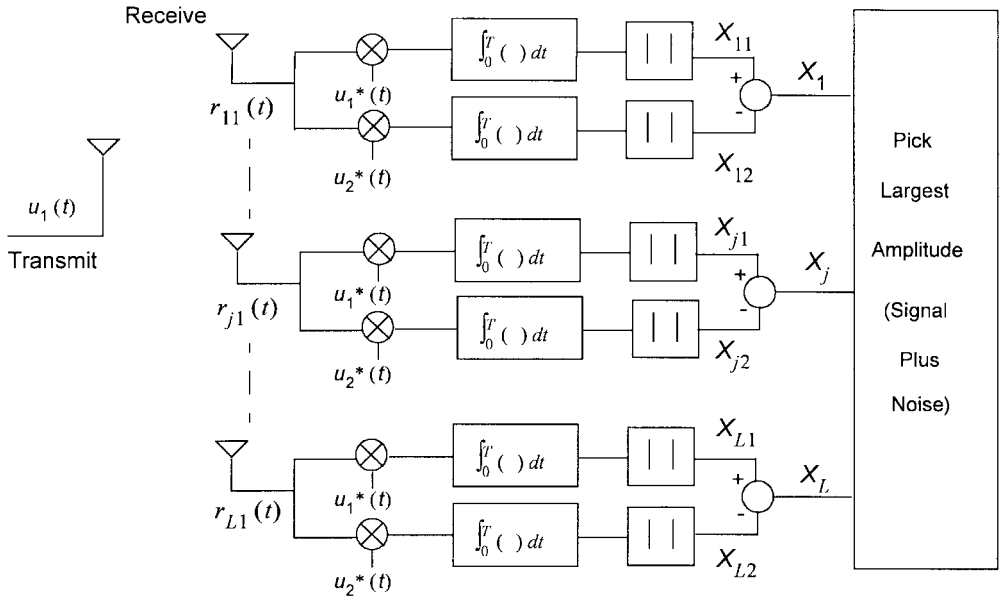

Fig. 2. Binary NCFSK $S+N$ Selection Receiver Model 2 showing $u_1(t)$ being transmitted for analysis purposes.

B. S + N Selection Receiver Model 2

This model is shown in Fig. 2. It differs from $S+N$ Selection Receiver Model 1, shown in Fig. 1, in that now a summing process occurs on each branch before invoking data recovery logic. To the best of the authors' knowledge, an analysis of the system shown in Fig. 2 has not yet been reported. The receiver bases its decision on the random variables $X_1,\cdots,X_L$ and, as in the case of the previous model, the analysis assumes the transmission of the low-pass equivalent signal $u_1(t)$. The output statistic from the jth branch is $X_j = X_{j1} - X_{j2} = |2\alpha_j + Y_{j1}| - |Y_{j2}|$ which, under static conditions, is the difference between a Rician- and a Rayleigh-distributed random variable. The complex Gaussian random variables Y_{jm}, $m=1,2$ were detailed above. An error occurs if $X_p<0$ and $|X_p|>\max|\{X_{j,j\neq p}\}|$, $j=1,2,\cdots,p,\cdots,L$. That is, an error occurs if, of the L statistics X_j, the one with the largest magnitude is negative. The average BER is written

$$\begin{aligned}P(e)_{\text{NCFSK}_{S+N\,\text{Model 2}}} &= \sum_{p=1}^{L}\Pr(\max|X_{j,j\neq p}|<|X_p|, X_p<0),\\ &\qquad j=1,2,\cdots,L\\ &= L\cdot\Pr(\max|X_{j,j\neq 1}|<|X_1|, X_1<0)\\ &= L\cdot\Pr\{(\max|X_{j,j\neq 1}|+X_1)<0\}\end{aligned}\tag{5}$$

which has solution

$$\begin{aligned}P(e)_{\text{NCFSK}_{S+N\,\text{Model 2}}} &= L\cdot\int_{-\infty}^{0}\left(\frac{-x_1e^{-x_1^2/2\sigma^2}}{\sigma^2(\overline{\gamma}_b+2)}+C_1\cdot e^{-x_1^2/2\sigma^2(\overline{\gamma}_b+2)}\right.\\ &\quad\cdot\left[\{1-Q(x_1C_2)\}\cdot\left\{1-\frac{x_1^2}{\sigma^2(\overline{\gamma}_b+2)}\right\}\right.\\ &\quad\left.+x_1\cdot\frac{C_2}{\sqrt{2\pi}}\cdot e^{-(x_1C_2)^2/2}\right]\Bigg)\\ &\quad\cdot\left(1-\left(\frac{\overline{\gamma}_b+1}{\overline{\gamma}_b+2}\right)e^{-x_1^2/2\sigma^2(\overline{\gamma}_b+1)}\right.\\ &\quad-\frac{e^{-x_1^2/2\sigma^2}}{\overline{\gamma}_b+2}-C_1x_1\cdot e^{-x_1^2/2\sigma^2(\overline{\gamma}_b+2)}\\ &\quad\left.\cdot[2-Q(x_1C_2)-Q(x_1C_3)]\right)^{L-1}dx_1\end{aligned}\tag{6}$$

following the technique detailed at Appendix A. In (6) the constants C_1, C_2, and C_3 are given by $C_1 = \sqrt{2\pi(\overline{\gamma}_b+1)/\sigma^2(\overline{\gamma}_b+2)^3}$, and $C_2 = \sqrt{(\overline{\gamma}_b+1)/\sigma^2(\overline{\gamma}_b+2)}$, and $C_3 = 1/\sqrt{\sigma^2(\overline{\gamma}_b+1)\,(\overline{\gamma}_b+2)}$, the variance is specified as $\sigma^2 = 2/\overline{\gamma}_b$, and the Q-function is defined as

$$Q(z)=\int_z^\infty\frac{e^{-t^2/2}}{\sqrt{2\pi}}dt.\tag{7}$$

Equation (6) is evaluated numerically.

C. S + N Selection Receiver Model 3

The $S+N$ Selection Receiver Model 3 is shown in Fig. 3. In contrast to $S+N$ Selection Receiver Model 2 (addressed above), now the envelopes are squared before being summed to form a branch output statistic. This detail is reflected in Fig. 3 by using the notation W vice X to label the branch output statistics. We have $W_j = W_{j1} - W_{j2} = |2\alpha_j + Y_{j1}|^2 - |Y_{j2}|^2$ which, under static conditions, is the difference between a noncentral and a central chi-square random variable, respectively, each with $n=2$ degrees of freedom. The complex Gaussian random variables Y_{jm}, $m=1,2$ were detailed above. Again, an error occurs if, of the L output statistics, the one with the largest magnitude is negative. We

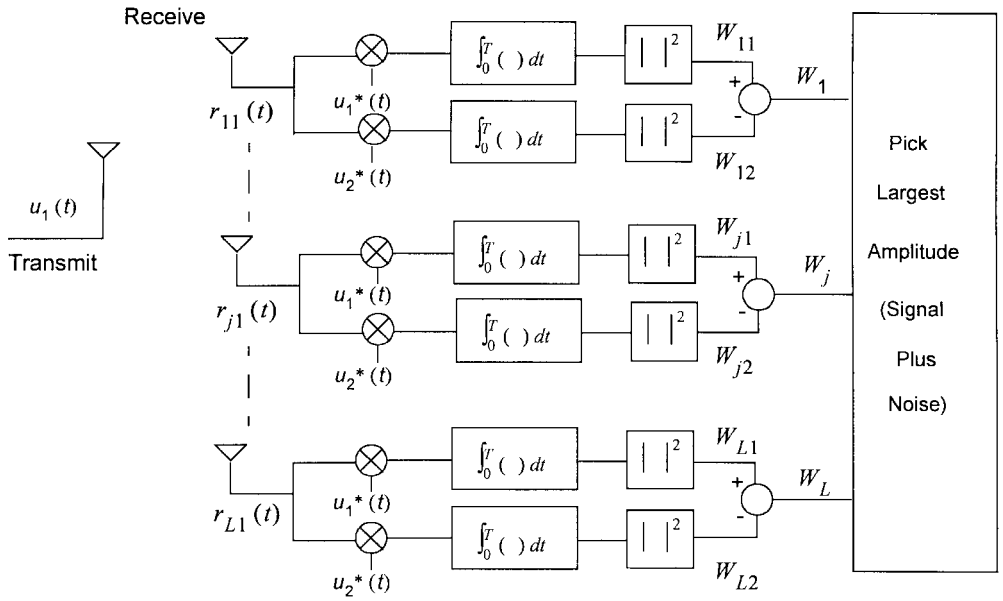

Fig. 3. Binary NCFSK $S+N$ Selection Receiver Model 3 showing $u_1(t)$ being transmitted for analysis purposes.

write

$$\begin{aligned} P(e)_{\text{NCFSK}_{S+N\text{ Model 3}}} &= \sum_{p=1}^{L} \Pr(\max|W_{j,j\neq p}| < |W_p|, W_p < 0), \\ &\qquad j = 1,2,\cdots,L \\ &= L \cdot \Pr(\max|W_{j,j\neq 1}| < |W_1|, W_1 < 0) \\ &= L \cdot \Pr\{(\max|W_{j,j\neq 1}| + W_1) < 0\} \end{aligned} \tag{8}$$

which has solution

$$\begin{aligned} P(e)_{\text{NCFSK}_{S+N\text{ Model 3}}} &= L \cdot \sum_{k=0}^{L-1} \binom{L-1}{k} \cdot \frac{(-1)^k}{(\overline{\gamma}_b+2)^{k+1}} \cdot \sum_{i=0}^{k} \binom{k}{i} \\ &\quad \cdot \frac{(\overline{\gamma}_b+1)^{i+1}}{\overline{\gamma}_b(k-i+1)+k+1}. \end{aligned} \tag{9}$$

To compute (9) from (8), exactly the same procedure is used as that which was used to compute (6) from (5) (see Appendix A). However, note that in this present case ($S+N$ Selection Receiver Model 3), the branch outputs are statistically described by the difference between a noncentral and a central chi-square random variable, as compared to $S+N$ Selection Receiver Model 2, where the difference between a Rician- and a Rayleigh-distributed random was required. This greatly facilitates the resulting mathematics and ultimately allows a closed-form solution (9) to describe $S+N$ Selection Receiver Model 3, unlike the solution (6) to $S+N$ Selection Receiver Model 2, which must be evaluated numerically.

III. NCFSK Results

We now discuss the performance of the receiver structures described above. Maximal ratio (MR) combining, square law combining, and equal gain (EG) combining curves are included for reference where applicable. First consider Fig. 4. The

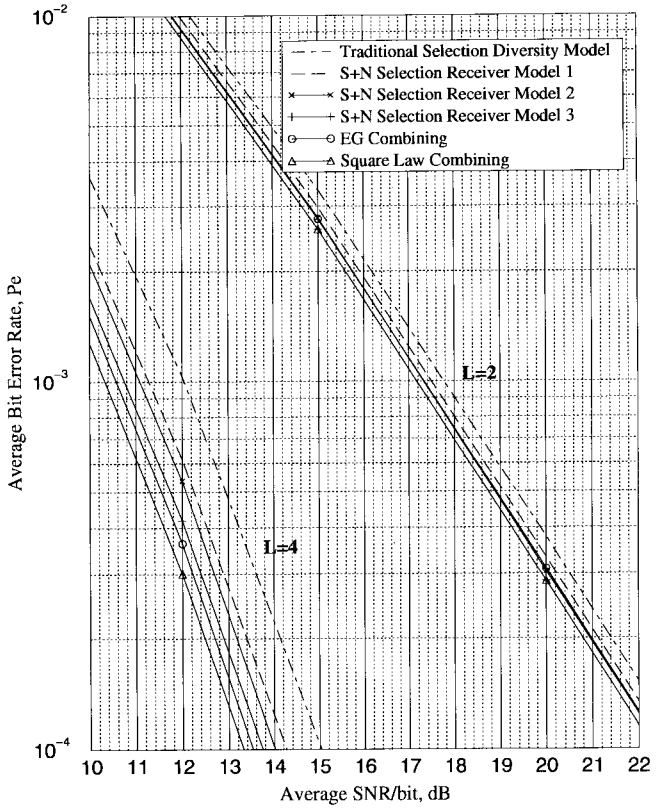

Fig. 4. Performance comparison of NCFSK receiver structures for $L=2$ and $L=4$ branch diversity.

abscissa is $\overline{\gamma}_b$ as defined in Section I (vice $L \cdot \overline{\gamma}_b$ as used in [4]). Distinct average BER differences between the NCFSK receiver systems, for each of two- and four-branch diversity, are evident. As an example, for dual diversity, for an average BER of 10^{-3}, the difference in required SNR per bit predicted by the Traditional Selection Diversity Model and each of $S+N$ Selection Receiver Models 1, 2, and 3 is 0.2, 0.4,

and 0.5 dB, respectively. For fourfold diversity the corresponding differences are 0.8, 1.0, and 1.2 dB, respectively. The performance difference between the Traditional Selection Diversity Model and $S+N$ Selection Receiver Model 1 is that which was reported in [4]; however, no explanation was offered for this result. Our treatment indicates that the latter model outperforms the former model because it (the latter) takes into account the statistical nature of the noise. That the difference becomes greater for higher orders of diversity can be attributed to the increased number of choices among statistically independent noise sources.

To the best of the authors' knowledge, the consideration of $S+N$ Selection Receiver Models 2 and 3 is new. Fig. 4 shows that, in fact, the dual diversity $S+N$ Selection Receiver Model 2 system performs identically to the EG combining system, while the dual diversity $S+N$ Selection Receiver Model 3 system performs identically to the square law combining system. This is expected intuitively for the dual diversity case because the sign of the sum of two algebraic summands is determined by the summand having largest magnitude. This is especially significant in that dual-diversity systems are by far the most common in current applications. For fourfold diversity, Fig. 4 shows that EG and square law combining outperform $S+N$ selection. The EG combining results were obtained using digital computer simulation. The $S+N$ Selection Receiver Model 2 results were obtained numerically using (6). All other results were obtained analytically using (1), (4), (9), and [10, eq. (14-4-15)] for the Traditional Selection Diversity Model, $S+N$ Selection Receiver Model 1, $S+N$ Selection Receiver Model 3, and square law combining, respectively. All analytical results have been confirmed by computer simulation.

Fig. 5 is provided to illustrate performance trends as the number of diversity branches increases. The average BER $P(e)$ is plotted against the order of diversity for each of the systems indicated. To produce Fig. 5, an average SNR per bit of 15 dB was chosen as being representative of the mobile communications environment. For other values of SNR per bit, the same performance trends are observed as those seen in Fig. 5 [6]. The results in Fig. 5 indicate that the $S+N$ Selection Receiver Models all perform increasingly better than the Traditional Selection Diversity Model as the order of diversity increases. Interestingly, there is little performance difference between $S+N$ Selection Receiver Models 1 and 2, with model 2 outperforming model 1. This is to be expected for the following reason. The most likely error situation for model 1 is that of a noise-only branch output having the largest magnitude which is slightly larger than the largest signal-plus-noise branch output. In this case the subtraction effected by receiver model 2 deemphasizes this branch relative to the other branches.

Fig. 6 compares selection combining to the optimum combining technique, MR combining [7], [8]. The (analytically established) performance of MR-combined NCFSK is presented in [8] and [9]. Fig. 6 shows the required SNR per bit over MR combining, for certain receiver structures discussed above, as the number of diversity branches increases. To produce Fig. 6, an average BER of $P(e)=10^{-3}$ was chosen.

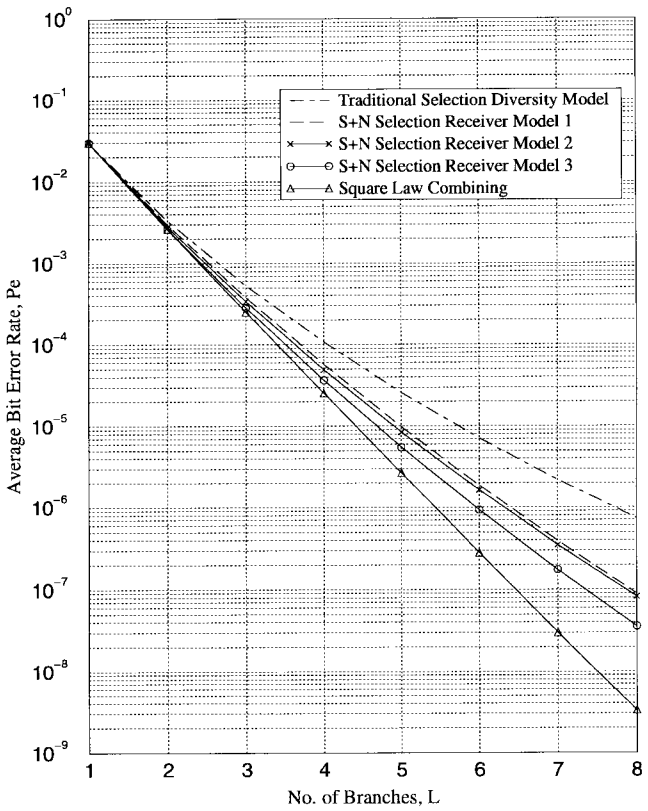

Fig. 5. Performances of NCFSK receiver structures, plotted for average SNR per bit = 15 dB, as the number of diversity branches grows.

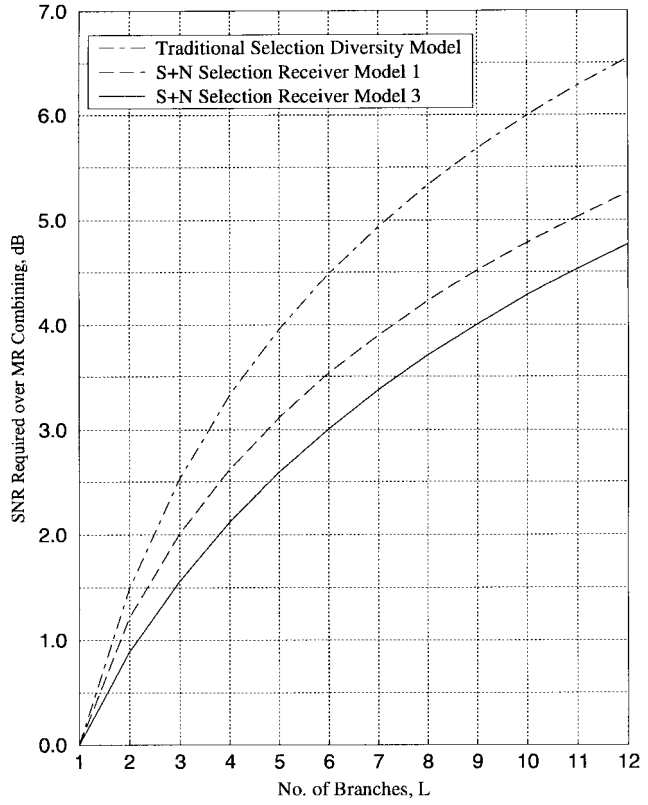

Fig. 6. Required SNR per bit over MR combining for various selection combining receiver structures and specified number of diversity branches. The average BER is $P(e)=10^{-3}$.

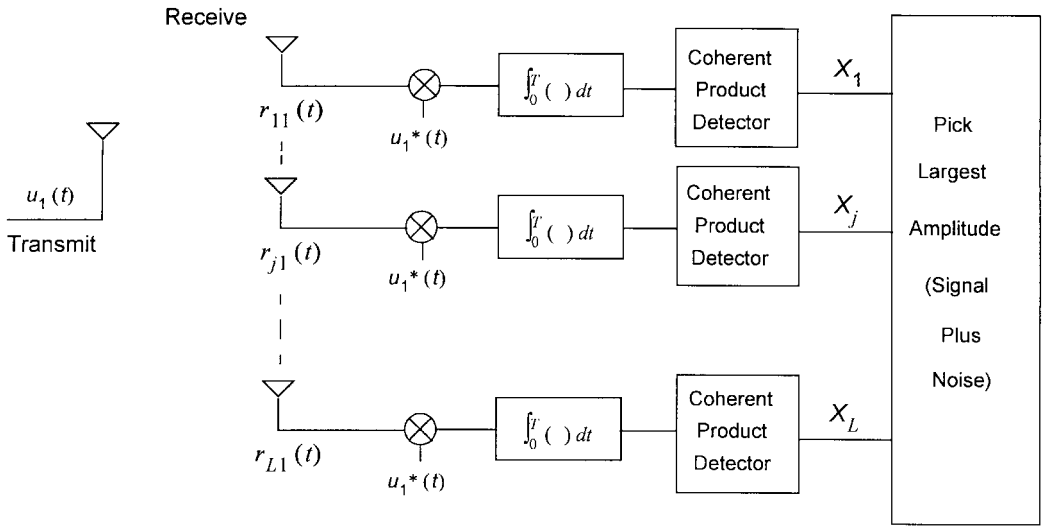

Fig. 7. Binary DPSK receiver model for $S+N$ selection showing $u_1(t)$ being transmitted for analysis purposes.

For different values of $P(e)$, the same performance trend is observed as that seen in Fig. 6 [6]. The MR combining curve is effectively the horizontal axis. When there is no diversity (i.e., $L=1$) all selection combining receiver structures perform identically and equal the performance of MR combining; thus, the SNR per bit required over MR combining is 0.0 dB for all three systems indicated. As the number of diversity branches increases, the selection-combining receiver structures are shown to deviate, in terms of performance, from the MR-combining curve. Note that the Traditional Selection Diversity Model gives the worst performance of the three in that it requires the most SNR per bit over MR combining to retain the average BER of 10^{-3}. The $S+N$ selection curves fall intermediately between the Traditional Selection Diversity Model and MR combining. Although they do not lose as much as the Traditional Selection Diversity Model, all selection diversity schemes lose substantially compared to MR combining as the diversity order increases.

IV. Extension to Binary DPSK

The use of DPSK signaling in conjunction with diversity combining is practical and desirable when the carrier phase does not change appreciably over two consecutive symbol durations [10]. With binary DPSK, antipodal signaling may be assumed so that only one matched filter per diversity branch is required, as illustrated in Fig. 7. We consider the product detector for demodulation. The output statistic for each branch is $X_j = \mathrm{Re}\{X_{jt2} \cdot X_{jt1}^*\}$, which may be written as $X_j = \mathrm{Re}\{(2\alpha_j + Y_{jt2}) \cdot (2\alpha_j + Y_{jt1}^*)\}$, where tx, $x = 1,2$ represents two consecutive time periods. The Y_{jtx}, $x = 1,2$ are i.i.d. complex Gaussian random variables with zero mean and variance $4/\overline{\gamma}_b$, and * denotes complex conjugation. For derivation of the $S+N$ selection system performance, the statistical characterization of the X_j is facilitated by application of the identity given in [9, eq. (8-2-1)]. The average BER $P(e)_{\mathrm{DPSK}_{S+N}}$ may be expressed as in (5) and thus evaluated using the technique of Appendix A. The result is

$$P(e)_{\mathrm{DPSK}_{S+N}} = L \cdot \sum_{k=0}^{L-1} \binom{L-1}{k} \cdot \frac{(-1)^k}{(2\overline{\gamma}_b+2)^{k+1}} \cdot \sum_{i=0}^{k} \binom{k}{i} \cdot \frac{(2\overline{\gamma}_b+1)^{i+1}}{2\overline{\gamma}_b(k-i+1)+k+1}. \tag{10}$$

In comparison, an analysis of the Traditional Selection Diversity Model for DPSK establishes the average BER as

$$P(e)_{\mathrm{DPSK}_{\mathrm{Trad}}} = \frac{1}{2} \cdot \sum_{i=1}^{L} \frac{i}{i+\overline{\gamma}_b} \tag{11}$$

which may be obtained by following exactly the technique given by Pierce [1] for NCFSK (as described in Section I) except that the time-invariant (static) channel-error rate is given by [10, eq. (14-3-9)] for DPSK vice [10, eq. (14-3-11)] for NCFSK. Note the similarity of (10) to (9) and the similarity of (11) to (1), the difference within each pair being a scaling of the SNR by a factor of two. This is the well-known 3-dB improvement in SNR performance of DPSK over NCFSK [9]. Similar performance trends (Figs. 5 and 6) were seen for DPSK [6] as were seen with NCFSK. Also consistent with the NCFSK results, DPSK $S+N$ selection (10) performs better than that predicted by the DPSK Traditional Selection Diversity Model (11), with the difference between the two, in average SNR per bit for $P_e = 10^{-3}$, being 0.6 dB for dual diversity and 1.2 dB for fourfold diversity [6]. For DPSK, EG combining is the optimum combining technique against which the performances of the former two techniques are compared. The analysis shows [6] that $S+N$ selection and EG combining [10, eq. (14-4-15)] actually perform identically for dual diversity. This is particularly interesting in that until now EG combining was thought to *uniquely* provide the best performance for DPSK diversity combining. To the authors' knowledge, these results are new and are not available elsewhere. For higher orders of diversity, EG combining outperforms $S+N$ selection combining.

V. Extension to Binary CPSK and CFSK

Estimation of carrier phase may be difficult or expensive in fading environments. Traditionally, MR or EG combining have been primarily considered in conjunction with coherent demodulation, and selection combining in conjunction with noncoherent demodulation. Advances in integrated circuits have resulted in the availability of coherent demodulation and receiver components of low cost. The combination of selection diversity with coherent demodulation is practical for systems such as packet data systems with the diversity branch selection being made on a block or packet duration basis. In this section the performances of selection diversity schemes operating with coherent demodulators are examined.

A. CPSK

We begin with binary antipodal CPSK signaling. As for the DPSK system considered above, only one matched filter per diversity branch is required so that a diagram of this system would be similar to Fig. 7, with appropriate modifications to reflect the coherency of this modulation technique (i.e., cophasing and no product detection). Under static conditions, the branch output statistics $X_j = 2\alpha_j + Z_j$ are Gaussian distributed where the Gaussian-distributed $Z_j, j = 1, 2, \cdots, L$ are i.i.d. with zero mean and variance $2/\overline{\gamma}_b$. The average BER $P(e)_{\mathrm{CPSK}_{S+N}}$ may be expressed as in (5) and evaluated using the technique of Appendix A to yield

$$P(e)_{\mathrm{CPSK}_{S+N}} = \int_{-\infty}^{0} \left\{ \int_0^\infty \frac{1}{\sigma\sqrt{2\pi}} e^{-(x_1-2\alpha_1)^2/2\sigma^2} \cdot 2\alpha_1 e^{-\alpha_1^2}\, d\alpha_1 \right\} \cdot \left\{ \int_0^\infty \left[Q\left(\frac{x_1+2\alpha_j}{\sigma}\right) + Q\left(\frac{x_1-2\alpha_j}{\sigma}\right) - 1 \right] \cdot 2\alpha_f e^{-\alpha_j^2}\, d\alpha_j \right\}^{L-1} dx_1 \quad (12)$$

which may be evaluated numerically. Note that $\sigma^2 = 2/\overline{\gamma}_b$.

As in the case of NCFSK and DPSK, the analysis of CPSK using the Traditional Selection Diversity Model follows the technique outlined in Pierce [1]; however, the process is sufficiently different mathematically that further detail is provided in Appendix B. The result is

$$P(e)_{\mathrm{CPSK}_{\mathrm{Trad}}} = \frac{1}{2} \cdot \sum_{k=0}^{L} (-1)^k \cdot \binom{L}{k} \cdot \sqrt{\frac{\overline{\gamma}_b}{\overline{\gamma}_b + k}}. \quad (13)$$

To the best of the authors' knowledge, (13) is a new result.

B. CFSK

As for NCFSK, the binary CFSK system requires two matched filters per diversity branch. Receiver structure block diagrams are similar to those of Figs. 1 and 2 with appropriate modifications to reflect the coherency of this modulation technique (i.e. cophasing and no envelope detectors). The output statistics from each branch are $X_{j1} = 2\alpha_j + Z_{j1}$ and $X_{j2} = Z_{j2}$, where the Gaussian random variables Z_{jm}, $m = 1, 2$ are i.i.d. with zero mean and variance $2/\overline{\gamma}_b$. Three systems, $S+N$ Selection Receiver Model 1, $S+N$ Selection Receiver Model 2, and the Traditional Selection Diversity Model, are discussed below.

In the CFSK $S+N$ Selection Receiver Model 1 system, the largest filter output is chosen for data recovery (similar to Fig. 1 for NCFSK). The average BER $P(e)_{\mathrm{CFSK}_{S+N\,\mathrm{Model\,1}}}$ is thus expressed as in (3) and has solution (following the technique in [4] for NCFSK)

$$P(e)_{\mathrm{CFSK}_{S+N\,\mathrm{Model\,1}}} = L \cdot \int_{-\infty}^{\infty} \left[\int_0^\infty \left[1 - Q\left(\frac{x-2\alpha_j}{\sigma}\right) \right] \cdot 2\alpha_j e^{-\alpha_j^2}\, d\alpha_j \right]^L \cdot \left[1 - Q\left(\frac{x}{\sigma}\right) \right]^{L-1} \cdot \frac{1}{\sigma\sqrt{2\pi}} e^{-x^2/2\sigma^2}\, dx \quad (14)$$

which is evaluated numerically. Note that $\sigma^2 = 2/\overline{\gamma}_b$.

For the CFSK $S+N$ Selection Receiver Model 2 system, the filter outputs are summed on each branch before choosing the largest amplitude (similar to Fig. 2 for NCFSK). Under static conditions, the branch output statistics $X_j = X_{j1} - X_{j2}$ are Gaussian distributed with variance $4/\overline{\gamma}_b$. The average BER $P(e)_{\mathrm{CFSK}_{S+N\,\mathrm{Model\,2}}}$ is written as in (5) and solves to the same equation as (12) except that now the variance is specified as $\sigma^2 = 4/\overline{\gamma}_b$ vice $\sigma^2 = 2/\overline{\gamma}_b$.

Finally, for the CFSK Traditional Selection Diversity Model, the analysis is identical to that presented in Appendix B for the CPSK Traditional Selection Diversity Model system except that now the variance is doubled ($\sigma^2 = 4/\overline{\gamma}_b$ vice $\sigma^2 = 2/\overline{\gamma}_b$). Thus, we may readily establish

$$P(e)_{\mathrm{CFSK}_{\mathrm{Trad}}} = \frac{1}{2} \cdot \sum_{k=0}^{L} (-1)^k \cdot \binom{L}{k} \cdot \sqrt{\frac{\overline{\gamma}_k}{\overline{\gamma}_b + 2k}} \quad (15)$$

which is obviously very similar to (13). To the best of the authors' knowledge, (15) is a new result.

C. Performance Results for CPSK/CFSK

Fig. 8 illustrates the performances of various CPSK receiver structures. For the coherent systems, MR combining is considered optimum [7], [8]; however, being more practical to implement, the performance of EG combining is the ideal against which the performances of the other combining techniques are compared. Again, the CPSK analysis shows [6] that the performance of a practical $S+N$ selection system (12) is not accurately portrayed by the Traditional Selection Diversity Model (13), the latter indicating a requirement for approximately 0.8 dB more average SNR per bit than the former for dual diversity, for an average BER of 10^{-3}. For fourfold diversity, the difference is 1.4 dB. The analysis also shows [6] that for the (most common) dual-diversity system, $S+N$ selection gives the same performance as EG combining (simulated). For fourfold diversity, EG combining outperforms $S+N$ selection. Note that the performance difference between the Traditional Selection Diversity Model and $S+N$ selection is actually greater for this coherent case than is the difference between the Traditional Selection Diversity Model and any of the $S+N$ selection models for the noncoherent cases (see Sections III and IV) discussed above. For CFSK, both $S+N$ Selection Receiver Models 1 (14) and 2 (12 with $\sigma^2 = 4/\overline{\gamma}_b$)

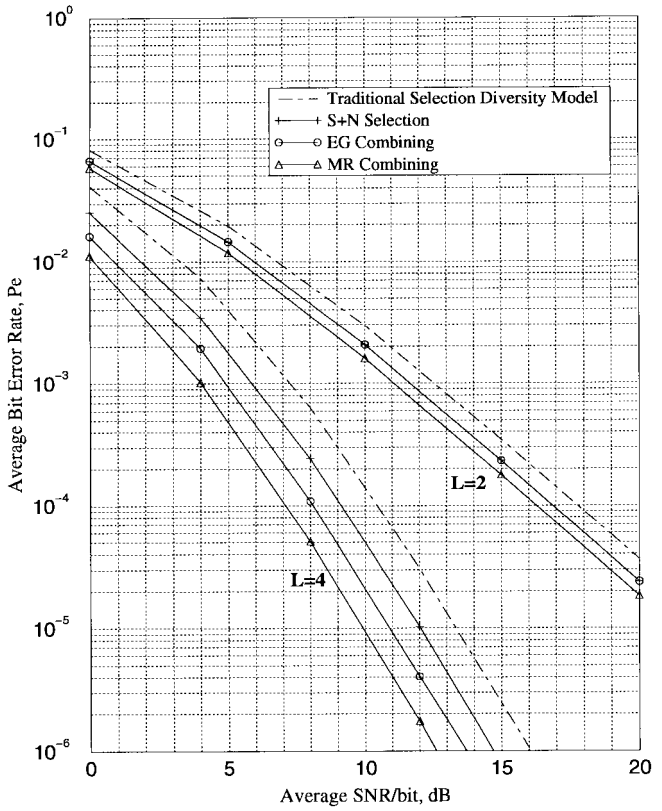

Fig. 8. Performance comparison of CPSK receiver structures for $L = 2$ and $L = 4$ branch diversity.

perform better than that predicted by the Traditional Selection Diversity Model (15), with $S + N$ Selection Receiver Model 2 giving the same performance as EG combining (simulated) for dual diversity. As an example, for dual diversity, for an average BER of 10^{-3}, the difference in required SNR per bit between the Traditional Selection Diversity Model and each of $S + N$ Selection Receiver Models 1 and 2 is 0.3 and 0.8 dB, respectively. For fourfold diversity, the respective differences are 0.7 and 1.2 dB. An illustrative performance comparison of CFSK receiver structures would be similar to that provided by Fig. 8 [6] except that, as expected, CFSK requires 3 dB more average SNR per bit than does CPSK to achieve the same BER for corresponding signaling schemes.

Of consequence, all EG combining results are dependent upon perfect phase estimates of the received signal, whereas the performance of an $S+N$ selection system is independent of any such phase estimate. Thus, it can be stated that the CPSK $S+N$ selection and CFSK $S+N$ Selection Receiver Model 2 systems actually outperform EG combining for dual diversity, where absolute knowledge of the combining carrier phases is not possible. Performance trends for CPSK and CFSK are similar to those presented in Figs. 5 and 6 for NCFSK [6]. The results for the coherent systems are consistent with those of the noncoherent systems detailed above.

VI. Conclusions

The efficacy of selection as a diversity combining technique has been revisited by comparing, for common binary signaling schemes, the performance of certain selection combining receiver structures against the performance of optimum combining schemes such as MR, EG, and square law combining as appropriate. A detailed analysis of binary NCFSK has been provided, with results extended to include binary DPSK, CPSK, and CFSK.

Specifically, by performing exact analyses of systems which select the branch with the largest $S+N$, it has been shown that the traditionally accepted selection diversity analysis, which focuses on selecting the branch with the largest SNR while assuming that the noise is a constant across all branches, produces a less-than-exact performance indication of a selection system. The reason for this discrepancy is that the analysis of the latter system includes the statistical nature of the noise while the former analysis does not. The performance difference between the two models increases as the number of diversity branches increases, due to an increased number of choices among statistically independent (Gaussian) noise samples. The results are significant in that many practical selection systems are implemented as selecting the largest $S + N$ for data recovery.

It was also shown that for each of DPSK and CPSK, the dual-diversity EG combining and $S + N$ selection systems perform identically. For each of NCFSK and CFSK, receiver structures which are equivalent when there is no diversity perform differently in a diversity environment. Certain dual-diversity NCFSK $S + N$ selection systems give the same performance as EG combining and square law combining. The performance of EG combining may also be achieved, using an $S+N$ selection scheme, for dual-diversity CFSK. These results are contingent upon perfect cophasing for the EG combining. In systems where estimates of the combining carrier phases contain noise, $S+N$ selection outperforms EG combining for dual diversity.

Appendix A

Here the method of computing (6) from (5) is provided. To express $P(e)_{\mathrm{NCFSK}_{S+N\,\mathrm{Model\,2}}}$ in useful form we first define the random variable R_j as $R_j = |X_j|$, $j = 1, 2, \cdots, L$, the random variable R as the maximum of the magnitudes $R = \max|X_{j,j\neq 1}| = \max\{R_{j,j\neq 1}\}$, and the random variable Z as the sum $Z = R + X_1$. Then (6) may be written as

$$P(e)_{\mathrm{NCFSK}_{S+N\,\mathrm{Model\,2}}} = L \cdot \Pr(Z < 0). \tag{A.1}$$

Note that R and X_1 are independent. Also note that $r_j \geq 0$, $j = 1, 2, \cdots, L$, and thus $r \geq 0$, while $x_1 \leq 0$. Since $\Pr(Z \leq z) = F_Z(z)$, it is evident from (A.1) that we must evaluate $F_Z(z)$ at $z = 0$. This is given by

$$\begin{aligned} F_z(0) &= \int_{-\infty}^{0} \int_{0}^{-x_1} f_{x_1}(x_1) f_R(r)\, dr\, dx_1 \\ &= \int_{-\infty}^{0} f_{x_1}(x_1)[F_R(-x_1) - F_R(0)]\, dx_1. \end{aligned} \tag{A.2}$$

To proceed with computing (A.2), the pdf $f_{x_1}(x_1)$ of X_1 for $x_1 \leq 0$ is required, as is the cdf $F_R(r)$ of $R = \max|X_{j,j\neq 1}|$. To establish these, the cdf of the random variable X_j is required. We derive this first.

The output statistic from the jth branch is $X_j = X_{j1} - X_{j2} = |2\alpha_j + Y_{j1}| - |Y_{j2}|$ which, under static conditions, is the difference between a Rician- and a Rayleigh-distributed random variable. Note that these random variables are independent. The complex Gaussian random variables Y_{jm}, $m = 1, 2$ are i.i.d. with zero mean and variance $4/\overline{\gamma}_b$. The Rician cumulative distribution function (cdf) is given by [10, eq. (2-1-142)] with the noncentrality parameter s^2 being defined at [10, eq. (2-1-119)] and detailed as $s^2 = 4\alpha_j^2$ in our particular case. Using the integral form of [10, eq. (2-1-122)] for $n = 2$ degrees of freedom, [10, eq. (2-1-142)] may be written as

$$F(x) = 1 - \int_{x/\sigma}^{\infty} x \cdot e^{-[(x^2/2)+\gamma_I]} \cdot \sum_{k=0}^{\infty} \frac{(\gamma_j x^2/2)^k}{(k!)^2} dx \quad \text{(A.3)}$$

where $\gamma_j = \alpha_j^2 \cdot \gamma_b$ is the SNR on branch j. To account for the fading, (A.3) is averaged across the pdf of γ_j, [10, eq. (14-3-5)]. This yields

$$F_{X_{j1}}(x_{j1}) = 1 - e^{-x_{j1}^2/2\sigma^2(\overline{\gamma}_b+1)}, \qquad x_{j1} \geq 0. \quad \text{(A.4)}$$

Continuing, the pdf of the Rayleigh distributed X_{j2} is given by [10, eq. (2-1-128)]

$$f_{X_{j2}}(x) = \frac{x_{j2}}{\sigma^2} \cdot e^{-x_{j2}^2/2\sigma^2}, \qquad x_{j2} \geq 0. \quad \text{(A.5)}$$

To describe the difference $X_j = X_{j1} - X_{j2}$, the joint density $f_{X_{j1},X_{j2}}(x_{j1}, x_{j2})$ is integrated across an appropriate region in the plane to determine the probability of that region. Since by definition $x_{j1} \geq 0$ and $x_{j2} \geq 0$, there are two convenient choices for regions of integration. For $x_j \leq 0$ we have

$$\begin{aligned} F_{X_j}(x_j) &= \int_{-x_j}^{\infty} \int_{0}^{x_j+x_{j2}} f_{X_{j1}}(x_{j1}) f_{X_{j2}}(x_{j2})\, dx_{j1}\, dx_{j2} \\ &= \int_{-x_j}^{\infty} f_{X_{j2}}(x_{j2}) \cdot [F_{X_{j1}}(x_j + x_{j2}) - F_{X_{j1}}(0)]\, dx_{j2}, \\ &\qquad x_j \leq 0 \end{aligned} \quad \text{(A.6a)}$$

and for $x_j \geq 0$ we have

$$\begin{aligned} F_{X_j}(x_j) &= \int_{0}^{\infty} \int_{0}^{x_j+x_{j2}} f_{X_{j1}}(x_{j1}) f_{X_{j2}}(x_{j2})\, dx_{j1}\, dx_{j2} \\ &= \int_{0}^{\infty} f_{X_{j2}}(x_{j2}) \cdot [F_{X_{j1}}(x_j + x_{j2}) - F_{X_{j1}}(0)]\, dx_{j2}, \\ &\qquad x_j \geq 0. \end{aligned} \quad \text{(A.6b)}$$

Substitution of (A.4) and (A.5) into each of (A.6a) and (A.6b), and evaluation of the integrals, produces

$$F_{X_j}(x_j) = \begin{cases} \dfrac{e^{-x_j^2/2\sigma^2}}{\overline{\gamma}_b + 2} + C_1 \cdot x_j \cdot e^{-x_j^2/2\sigma^2(\overline{\gamma}_b+2)} \\ \qquad \cdot \{1 - Q(x_j C_2)\}, \qquad x_j \leq 0 \quad \text{(A.7a)} \\ 1 - \left(\dfrac{\overline{\gamma}_b + 1}{\overline{\gamma}_b + 2}\right) e^{-x_j^2/2\sigma^2(\overline{\gamma}_b+1)} \\ \qquad + C_1 \cdot x_j \cdot e^{-x_j^2/2\sigma^2(\overline{\gamma}_b+2)} Q(x_j C_3), \\ \qquad x_j \geq 0 \quad \text{(A.7b)} \end{cases}$$

which is the cdf of the random variable X_j. The constants are detailed in Section II-B. Equation (A.7) is now used to establish the components of (A.2). By taking the derivative of (A.7a) and setting $j = 1$, we obtain

$$\begin{aligned} f_{X_1}(x_1) = {} & \frac{-x_1 e^{-x_1^2/2\sigma^2}}{\sigma^2(\overline{\gamma}_b + 2)} + C_1 \cdot e^{-x_1^2/2\sigma^2(\overline{\gamma}^2+2)} \\ & \cdot \left[\{1 - Q(x_1 C_2)\} \cdot \left\{ 1 - \frac{x_1^2}{\sigma^2(\overline{\gamma}_b + 2)} \right\} \right. \\ & \left. + x_1 \frac{C_2}{\sqrt{2\pi}} \cdot e^{-(x_1 C_2)^2/2} \right], \qquad x_1 \leq 0 \end{aligned} \quad \text{(A.8)}$$

which gives the first factor in the integrand in (A.2). For the second factor in the integrand in (A.2), the distribution of $R = \max\{R_{j,j\neq 1}\}$ is required. Since the X_j, and thus the R_j, are i.i.d., we have $F_R(r) = [F_{R_j}(r_j)]^{L-1}$, where $F_{R_j}(r_j)$ is computed as

$$\begin{aligned} F_{R_j}(r_j) &= \Pr(R_j \leq r_j) \\ &= \Pr(-r_j \leq X_j \leq 0) + \Pr(0 \leq X_j \leq r_j) \\ &= F_{X_j}(r_j) - F_{X_j}(-r_j). \end{aligned} \quad \text{(A.9)}$$

Using (A.7b) evaluated at r_j, and (A.7a) evaluated at $-r_j$, in (A.9) as indicated yields

$$\begin{aligned} F_{R_j}(r_j) = {} & 1 - \left(\frac{\overline{\gamma}_b + 1}{\overline{\gamma}_b + 2}\right) e^{-r_j^2/2\sigma^2(\overline{\gamma}_b+1)} - \frac{e^{-r_j^2/2\sigma^2}}{\overline{\gamma}_b + 2} \\ & + C_1 r_j \cdot e^{-r_j^2/2\sigma^2(\overline{\gamma}_b+2)} [Q(r_j C_2) + Q(r_j C_3)], \\ & r_j \geq 0. \end{aligned} \quad \text{(A.10)}$$

Finally, use of (A.8) and (A.10) in (A.2), and substitution of the solution into (A.1), produces (6).

Appendix B

Here, the average BER for the Traditional Selection Diversity Model using CPSK signaling $P(e)_{\text{CPSK}_{\text{Trad}}}$ is computed. Following the technique outlined in Pierce [1] for NCFSK, the static channel-error rate $P(\gamma)$ is averaged over the pdf $f(\gamma)$ of the largest SNR γ of the L branches. That is

$$P(e)_{\text{CPSK}_{\text{Trad}}} = \int_{-\infty}^{\infty} P(\gamma) \cdot f(\gamma)\, d\gamma. \quad \text{(B.1)}$$

The error rate of CPSK without fading is well known [10, eq. (14-3-2)], as is the pdf $f(\gamma)$ for Rayleigh fading [10, eq. (14-3-5)]. Substitution of these in (B.1) yields

$$\begin{aligned} P(e)_{\text{CPSK}_{\text{Trad}}} = {} & \int_{0}^{\infty} Q(\sqrt{2\gamma}) \cdot L \cdot (1 - e^{-\gamma/\overline{\gamma}_b})^{L-1} \\ & \cdot \frac{1}{\overline{\gamma}_b} e^{-\gamma/\overline{\gamma}_b}\, d\gamma. \end{aligned} \quad \text{(B.2)}$$

With application of [11, eq. (7.1.6)] and the binomial theorem, (B.2) is written

$$\begin{aligned} P(e)_{\text{CPSK}_{\text{Trad}}} = {} & \frac{1}{2} - \frac{L}{\sqrt{\pi}} \cdot \sum_{k=0}^{L-1} (-1)^k \binom{L-1}{k} \\ & \cdot \sum_{i=0}^{\infty} \frac{2^{i+1}}{(2i+1)!!} \cdot \frac{1}{\overline{\gamma}_b} \\ & \cdot \int_{0}^{\infty} \gamma^{2(i+1)} \cdot e^{-\gamma^2[\overline{\gamma}_b + (k+1)]/\overline{\gamma}_b}\, d\gamma. \end{aligned} \quad \text{(B.3)}$$

Applying [12, eq. (3.461.2)] to the integral in (B.3), and using [11, eq. (3.1.10)] (geometric series), we obtain

$$P(e)_{\mathrm{CPSK_{Trad}}} = \frac{1}{2} - \frac{L}{2} \cdot \sum_{k=0}^{L-1} \frac{(-1)^k}{1+k} \cdot \binom{L-1}{k} \cdot \sqrt{\frac{\overline{\gamma}_b}{\overline{\gamma}_b + (k+1)}} \tag{B.4}$$

which may be manipulated into the form given at (13).

REFERENCES

[1] J. N. Pierce, "Theoretical diversity improvement in frequency-shift keying," *Proc. IRE*, vol. 46, pp. 903–910, May 1958.

[2] W. C. Jakes, Ed., *Microwave Mobile Communications*. Piscataway, NJ: IEEE Press, 1974.

[3] F. E. Bond and H. F. Meyer, "The effect of fading on communication circuits subject to interference," *Proc. IRE*, vol. 45, pp. 636–642, May 1957.

[4] G. Chyi, J. G. Proakis, and C. M. Keller, "On the symbol error probability of maximum-selection diversity reception schemes over a Rayleigh fading channel," *IEEE Trans. Commun.*, vol. 37, pp. 79–83, Jan. 1989.

[5] G. F. Montgomery, "Message error in diversity frequency-shift reception," *Proc. IRE*, vol. 42, pp. 1184–1187, July 1954.

[6] E. A. Neasmith, "Selection diversity with binary signalling schemes," M.Sc. thesis, Queen's Univ., Kingston, Ont., Canada, July 1996.

[7] D. G. Brennan, "Linear diversity combining techniques," *Proc. IRE*, vol. 47, pp. 1075–1102, June 1959.

[8] S. Stein, "Fading channel issues in system engineering," *IEEE J. Select. Areas. Commun.*, vol. SAC-5, pp. 68–89, Feb. 1987.

[9] M. Schwartz, W. R. Bennett, and S. Stein, *Communication Systems and Techniques*. New York: McGraw-Hill, 1966.

[10] J. G. Proakis, *Digital Communications*, 3rd ed. New York: McGraw-Hill, 1995.

[11] M. Abramowitz and I. A. Stegun, Eds., *Handbook of Mathematical Functions* (Applied Mathematics Series 55). Washington, DC: NBS, 1964.

[12] I. S. Gradshteyn and I. M. Ryzhik, *Table of Integrals, Series and Products*. New York: Academic, 1965.

Elisabeth A. Neasmith (M'93) received the B.Sc. degree in electrical engineering from the Royal Military College of Canada, Kingston, Ont., in 1988, and the M.Sc. degree in electrical engineering from Queen's University, Kingston, Ont., Canada, in 1996.

She is currently serving in the Canadian Armed Forces as Head of Spectrum Engineering with the National Defence Headquarters, Ottawa, Ont., Canada.

Norman C. Beaulieu (S'82–M'84–SM'89), for photograph and biography, see this issue, p. 665.